Theoretical Considerations on Inelastic Electron Scattering at High Energies

HUNG CHENG*
Department of Mathematics, Massachusetts Institute of Technology, Cambridge, Massachusetts 02139
AND
TAI TSUN WU
Gordon McKay Laboratory, Harvard University, Cambridge, Massachusetts 02138
(Received 24 March 1969)

Physical arguments are presented for the conjecture that, compared with photoproduction and hadronic production, the difficulty in making large transverse momentum transfers at high energies is much less in electroproduction processes when the virtual photon is far off the mass shell. Model calculations are carried out to verify this result. In particular, in the c.m. systems of the outgoing hadrons, the angular distribution of the vector meson produced by the reactions $e^-+p\rightarrow e^-+p+\rho^0$ (or φ, or ω) is less peaked in the forward direction at high energies when the virtual photon is further off the mass shell. This and other possible experimental tests are discussed. This reduction of the forward peaks also makes electroproduction processes a fertile ground for testing statistical theories of high-energy collisions.

1. INTRODUCTION

IN this paper, we consider the inelastic electron scattering process

$$e^-+p\rightarrow e^-+B, \tag{1.1}$$

where B is a hadron system with total mass $\sqrt{s}$. Because of the smallness of the fine-structure constant, we shall take care of one-photon exchange only. Let m and m_p be the masses of the electron and the proton, respectively, E and E' be the energies of the incident and the scattered electron, respectively, $\nu=E-E'$ be the energy loss, k_μ the four-momentum of the exchange photon, and θ be the scattering angle for the electron in the laboratory system, then

$$k^2=2m^2-2EE'+2(E^2-m^2)^{1/2}(E'^2-m^2)^{1/2}\cos\theta \tag{1.2}$$

and

$$s=m_p^2+2m_p\nu+k^2. \tag{1.3}$$

The metric used is $(1,-1,-1,-1)$ so that k^2 is negative (spacelike). We are in essence considering the scattering of a virtual photon with negative mass squared ($=k^2$) by a proton, the total c.m. energy squared of the photon-proton system being s.

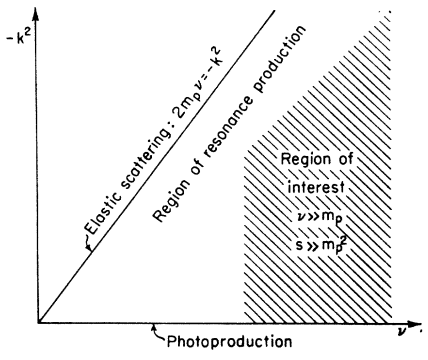

FIG. 1. Region of interest in the $(-k^2, \nu)$ plane.

We shall study here the case where both E' and ν are very large, say, a few BeV, then (1.2) is approximately

$$k^2=-2EE'(1-\cos\theta). \tag{1.4}$$

When $2m_p\nu=-k^2$, (1.3) shows that $s=m_p^2$, and the scattering amplitude is related to the proton form factor. When $2m_p\nu\geq -k^2+2m_p\mu+\mu^2$, where μ is the pion mass, pion production becomes possible. When $\nu\rightarrow\infty$, with k^2 fixed, we are dealing with high-energy virtual photon-proton scattering. The division of the kinematic space $(-k^2, \nu)$ is drawn in Fig. 1. We shall be interested in the region where s is large, $-2m_p\nu/k^2$ taking any value greater than one.

2. PHYSICAL PICTURE

We shall attempt to find the physical picture underlying the photon-proton scattering in the region of interest. It is helpful to start the discussion in a region of the $(-k^2, \nu)$ plane where some physical facts have been established. The positive ν axis is well suited for this purpose. This is because we have a real photon when $k^2=0$, and are dealing with the process of photoproduction.

We therefore first summarize some of the experimental as well as theoretical informations on high-energy production processes. On the experimental side, we know that:

(i) In the case of photoproduction, where $k^2=0$, a wealth of experimental facts are available on single-particle production processes. For example, the processes $\gamma+p\rightarrow\rho^0+p$ and $\gamma+p\rightarrow\varphi+p$ have been measured.[1] It was found that both of these processes are sharply peaked in the forward direction; more precisely $d\sigma/dt=d\sigma/dt|_{t=0}e^{Bt+Ct^2}$, where B is around

* Work supported in part by the National Science Foundation.

[1] W. G. Jones, D. Kreinick, R. Anderson, D. Gustavson, J. Johnson, D. Ritson, F. Murphy, M. Gettner, and R. Weinstein, Phys. Rev. Letters 21, 586 (1968).

8–10 $(\text{BeV}/c)^{-2}$ for ρ^0 production and is around 4.5–8 $(\text{BeV}/c)^{-2}$ for φ production.

(ii) In other single-particle production processes not involving photons such as $\pi^{\pm}+p \to \pi^{\pm}+N^*(1.4)$ and $p+p \to p+N^*(1.4)$, the angular distribution is given by $d\sigma/dt = d\sigma/dt|_{t=0} e^{Bt}$, with B ranging from 12.1 to 18.3 $(\text{BeV}/c)^{-2}$ for the various processes.[2]

(iii) In multiparticle production processes, such as $p+p \to \pi^{\pm}$ (or $K^{\pm}$)+other hadrons (undetected), the differential production cross section $d^2\sigma/(d\Omega dp)$ also peaks like $e^{-BP_\perp^2}$, where $P_\perp$ is the transverse momentum of the produced particle, with B ranging from 2.7 to 3.5 for the various processes.[3]

On the theoretical side, various models have been proposed. In particular, the rapid decrease of the differential cross section off the forward direction is seen to be related to the difficulty of transferring transverse momentum by particles acting as an extended object.[4] On this basis, we expect that even though there is not much direct experimental evidence,[5] the multiparticle photoproduction processes such as $\gamma+p \to \pi$ (or K) + other hadrons (undetected) must also show the same qualitative behavior as in (iii) above.

Recently, high-energy elastic scattering processes in quantum electrodynamics, such as $\gamma+p \to \gamma+p$, have been investigated.[6] Generalization to processes like $\gamma+p \to \rho^0+p$ can be made. The differential cross section is found to be peaked in the forward direction, with a width determined by the mass of the intermediate-state particles. The following physical picture is evident from the above investigation: Each particle exhibits a structure represented by its "impact factor," and the diffraction scattering proceeds through the exchange of vector mesons whose momenta are predominantly transverse in the c.m. system. Roughly speaking, the impact factor serves as a generalized form factor for multi-vector-meson exchanges. The dominant contribution to the total cross section is from the region where the intermediate-state particles have small transverse momenta. This is consistent with (i), (ii), and (iii) described above.

We have seen therefore that the differential production cross sections are strongly peaked in the forward direction. This is not only true in γp but also in πp and pp collisions, and is therefore not related to the massless nature ($k^2=0$) of the photon. Returning to the $(-k^2, \nu)$ plane for photon-proton scattering, we therefore expect that the production differential cross sections be strongly peaked in the region $\nu \to \infty$ with $-k^2$ held fixed.

Having described the γp scattering near the ν axis ($-k^2$ finite), we go to the other extreme case when $-k^2 \to \infty$, with $-2m_p\nu/k^2$ fixed at a value greater than one. In other words, we study the high-energy scattering process $s \to \infty$, with the photon having a negative mass squared comparable to s. In this case the photon is highly off-mass-shell, and by the uncertainty principle it must be extremely short-lived. There is then very little time for the photon to develop a structure through creation and annihilation processes. The diffraction mechanism is thereby weakened and the diffraction peak is flattened. Other competing processes become more important, and a completely different physical picture takes over. Because of the pointlike nature of the photon in this limit, it is now easier to transfer transverse momentum.

Finally, let us make an interpolation between the diffraction case $s \to \infty$, $-k^2$ held finite and the extreme case $s \to \infty$, $-k^2/(2m_p\nu)$ held finite. In order to make a smooth connection, the diffraction peak must be broadened and flattened as $-k^2$ increases. Indeed, the spread in $p_\perp^2$ must be of the order of $-k^2$ from dimensional arguments, when $-k^2$ is larger than the squares of the meson masses. A model calculation in Secs. 4 and 5, in fact, confirms this point.

Some considerations on the statistical model of Fermi[7,8] are given in Appendix A.

3. EXPERIMENTAL TESTS

We suggest some experiments relevant to the semiquantitative idea of Sec. 2.

A. Electroproduction of ρ^0

Consider first

$$e^-+p \to e^-+p+\rho^0. \tag{3.1}$$

When the mass of the $p-\rho^0$ system is large, ρ^0 is produced by the diffraction of the virtual photon. In the limit of photoproduction (i.e., when $k^2=0$), the angular distribution for ρ^0 is approximately e^{8t}, as already mentioned.[1] This angular distribution is strongly peaked in the forward direction. More generally, for the process (3.1), we expect, from the consideration Sec. 2, that the angular distribution of ρ^0 in the $p\rho^0$ system is less strongly peaked if $|k^2|$ is larger. More specifically, if we assume an exponential angular

[2] K. J. Foley, R. S. Jones, S. J. Lindenbaum, W. A. Love, S. Ozaki, E. D. Platner, C. A. Quarles, and E. H. Willen, Phys. Rev. Letters **19**, 397 (1967).

[3] L. G. Ratner, K. W. Edwards, C. W. Akerlof, D. G. Crabb, J. L. Day, A. D. Krisch, and M. T. Lin, Phys. Rev. Letters **18**, 1218 (1967).

[4] T. T. Wu and C. N. Yang, Phys. Rev. **137B**, 708 (1965).

[5] Some information can be obtained from the SLAC beam survey: S. M. Flatte, R. A. Gearhart, T. Hauser, J. J. Murray, R. Morgado, M. Peters, P. R. Klein, L. H. Johnston, and S. G. Wojcicki, Phys. Rev. Letters **18**, 366 (1967); A. Boyarski, F. Bulos, W. Busza, D. Coward, R. Diebold, J. Litt, A. Minten, B. Richter, and R. Taylor, *ibid.* **18**, 363 (1967).

[6] H. Cheng and T. T. Wu, Phys. Rev. (to be published). These papers are hereafter referred to as I, II, III, and IV. A summary is given in H. Cheng and T. T. Wu, Phys. Rev. Letters **22**, 666 (1969).

[7] E. Fermi, Prog. Theoret. Phys. **5**, 570 (1950).

[8] R. Hagedorn, Nuovo Cimento **15**, 434 (1960); G. Fast and R. Hagedorn, *ibid.* **27**, 208 (1963); G. Fast, R. Hagedorn, and L. W. Jones, *ibid.* **27**, 856 (1963); H. Bethe, *ibid.* **33**, 1167 (1964); R. Hagedorn, *ibid.* **35**, 216 (1965).

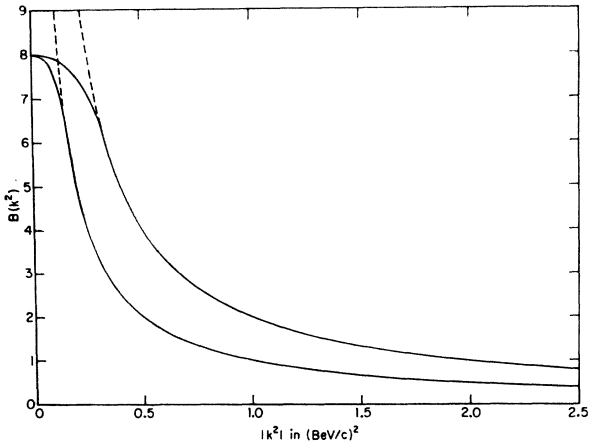

FIG. 2. Widening of angular distribution for the electroproduction of ρ^0. [The ρ^0 distribution is assumed to be of the form $\exp(B(k^2)t)$.]

distribution[9]

$$e^{B(k^2)t}, \tag{3.2}$$

then $B(k^2)$ is a decreasing function of $-k^2$. Here $-t$ is always the square of the four-momentum transfer between the photon (real or virtual) and the ρ meson.

Let us attempt to guess in more detail how $B(k^2)$ behaves. When k^2 is large, the most important scale must be k^2 itself. Therefore, for large k^2, by dimensional arguments[10]

$$B(k^2)\sim\text{const}(-k^2)^{-1}. \tag{3.3}$$

Interpolation between (3.3) and the photoproduction data gives very roughly the curves of Fig. 2, where the constant in (3.3) is taken to be 1 and 2.

Similar broadening is, of course, also expected for

$$e^-+p\rightarrow e^-+p+\varphi$$
and
$$e^-+p\rightarrow e^-+p+\omega. \tag{3.4}$$

It is an interesting question to ask whether there is also a broadening in the process $e^-+p\rightarrow e^-+n+\pi^+$, for example.

B. Electroproduction of pions

We next consider

$$e^-+p\rightarrow e^-+\pi^\pm+\text{other hadrons (not detected)}. \tag{3.5}$$

Again, in the c.m. system of all the hadrons, we expect the pion distribution to be more peaked for smaller $|k^2|$. The argument of Sec. 3 A can also be applied to get a very rough estimate of its broadening. Generalization to $K^\pm$ instead of $\pi^\pm$ is immediate.

C. Others

Suppose the hadron system B consists of a number of particles, and we detect two of them, say B_1 and B_2. Assume that B_1 and B_2 do not form a resonance, and consider their angular correlation. More precisely, for large $|k^2|$, we ask what is the characteristic scale for transverse momentum in the angular correlation of B_1 and B_2. One possible candidate is $|k^2|^{1/2}$, but the model calculation of the next sections indicates that this scale is perhaps much smaller, say $\frac{1}{2}$ BeV/c.

We therefore propose as an interesting experiment the measurement of

$$e^-+p\rightarrow e^-+\pi^\pm+\pi^\pm+\text{other hadrons}, \tag{3.6}$$

to study the angular correlation between like pions for large $|k^2|$.

4. DELBRÜCK SCATTERING OFF THE MASS SHELL

In order to substantiate the semiquantitative agruments presented above, we propose to carry out several model calculations in this and the following sections. In this section, we study forward Delbrück scattering in quantum electrodynamics at high energies with the transverse photon off the mass shell. We shall see that as the photon goes off the mass shell, the important scale for transverse momentum transfer shifts from the electron mass to the (imaginary) "photon mass." This implies in particular that the difficulty of making large transverse momentum transfers is lessened when the photon is far off the mass shell. The similar case of forward Delbrück scattering for a longitudinal photon is discussed in Sec. 5.

A. Formulation

We consider the two Feynman-Dyson diagrams shown in Fig. 3. The analysis of these diagrams follow rather closely our previous work for real photons[6] and is somewhat simplified by the restriction to forward directions. (A nonvanishing photon mass λ for the two internal photon lines shall be retained throughout.) Similar to (III 2.1) and (III 2.2), the contributions of the diagrams in Fig. 3 to the matrix elements of Delbrück scattering are, respectively,

$$\mathfrak{M}_1^{(D)}=2i(2\pi)^{-7}e^6Z^2\int d^4p\,d^3q[(k+p)^2-m^2]^{-1}$$
$$\times(p^2-m^2)^{-2}[(p+q)^2-m^2]^{-1}[\mathbf{q}^2+\lambda^2]^{-2}$$
$$\times\text{Tr}\gamma_i(\not p+m)\gamma_0(\not p+\not q+m)\gamma_0(\not p+m)$$
$$\times\gamma_j(\not k+\not p+m) \tag{4.1}$$

[9] We restrict ourselves to the contribution of the transverse photon. Even for the transverse photon, there is no compelling reason for exponential dependence on t.

[10] We have here assumed the absence of logarithmic terms. See Sec. 8.

and

$$\mathfrak{M}_2^{(D)}=i(2\pi)^{-7}e^6Z^2\int d^4p\,d^3q\,[(\tfrac{1}{2}k-p-\tfrac{1}{2}q)^2-m^2]^{-1}$$
$$\times[(\tfrac{1}{2}k-p+\tfrac{1}{2}q)^2-m^2]^{-1}[(-\tfrac{1}{2}k-p+\tfrac{1}{2}q)^2-m^2]^{-1}$$
$$\times[(-\tfrac{1}{2}k-p-\tfrac{1}{2}q)^2-m^2]^{-1}(\mathbf{q}^2+\lambda^2)^{-2}$$
$$\times\mathrm{Tr}\gamma_i(-\tfrac{1}{2}\boldsymbol{k}-\boldsymbol{p}-\tfrac{1}{2}\boldsymbol{q}+m)\gamma_0(-\tfrac{1}{2}\boldsymbol{k}-\boldsymbol{p}+\tfrac{1}{2}\boldsymbol{q}+m)$$
$$\times\gamma_j(\tfrac{1}{2}\boldsymbol{k}-\boldsymbol{p}+\tfrac{1}{2}\boldsymbol{q}+m)\gamma_0(\tfrac{1}{2}\boldsymbol{k}-\boldsymbol{p}-\tfrac{1}{2}\boldsymbol{q}+m). \quad (4.2)$$

Note that, compared with the notation of Ref. 6, $r_1=0$ and $r_2=k$. Moreover, (III 2.9) and (III 2.11) hold here.

Attention is immediately shifted to a generalization of the considerations of IV. Analogous to (IV 2.1), (IV 2.2), and (IV 2.27), we define

$$g^\gamma(\mathbf{q}_\perp)=\lim_{\omega\to\infty}(2\pi)^{-1}\int_{-\infty}^{\infty}dq_3\frac{R_1+R_2}{\omega}, \quad (4.3)$$

where

$$R_1=2(2\pi)^{-4}e^4\int d^4p[(k+p)^2-m^2]^{-1}$$
$$\times(p^2-m^2)^{-2}[(p+q)^2-m^2]^{-1}(8p_0^2)$$
$$\times(4p_ip_j+2p_ik_j+2k_ip_j-\delta_{ij}k^2) \quad (4.4)$$

and

$$R_2=(2\pi)^{-4}e^4\int d^4p[(\tfrac{1}{2}k-p-\tfrac{1}{2}q)^2-m^2]^{-1}$$
$$\times[(\tfrac{1}{2}k-p+\tfrac{1}{2}q)^2-m^2]^{-1}[(-\tfrac{1}{2}k-p+\tfrac{1}{2}q)^2-m^2]^{-1}$$
$$\times[(-\tfrac{1}{2}k-p-\tfrac{1}{2}q)^2-m^2]^{-1}\{2\omega^2[-(2p-q)_i(2p+q)_j$$
$$+\delta_{ij}(2q^2+k^2)+k_ik_j]-8\omega p_0(-k_iq_j+q_ik_j)$$
$$+8p_0^2[-k_ik_j+(2p+q)_i(2p-q)_j-\delta_{ij}k^2]\}. \quad (4.5)$$

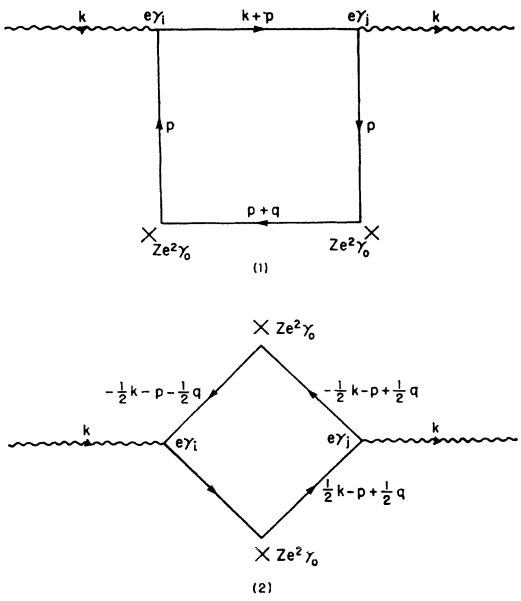

FIG. 3. Sixth-order diagrams for Delbrück scattering of a virtual photon.

With this definition of the photon impact factor, the asymptotic behavior of the matrix element for Delbrück scattering in the forward direction as given by (4.1) and (4.2) is, when $\omega\to\infty$,

$$\mathfrak{M}_0^{(D)}=\mathfrak{M}_1^{(D)}+\mathfrak{M}_2^{(D)}$$
$$\sim i\omega(2\pi)^{-2}e^2Z^2\int d\mathbf{q}_\perp(\mathbf{q}_\perp^2+\lambda^2)^{-2}g^\gamma(\mathbf{q}_\perp). \quad (4.6)$$

When the photon is transverse, $k_i=k_j=0$ and hence almost half of the terms in (4.4) and (4.5) vanish.

The procedure described in detail in Sec. 4 of IV can be followed step by step. We obtain the following result, similar to (IV 4.12), for $g^\gamma(\mathbf{q}_\perp)$, the photon impact factor off the mass shell in the forward direction:

$$g^\gamma(\mathbf{q}_\perp)=-\tfrac{1}{2}\pi^{-3}e^4\int d\mathbf{p}_\perp\int_0^1 dA\{A(1-A)$$
$$\times(2p_{\perp i}p_{\perp j}-\tfrac{1}{2}\delta_{ij}k^2)[\mathbf{p}_\perp^2+m^2-A(1-A)k^2]^{-2}$$
$$-[\tfrac{1}{4}\mathbf{q}_\perp^2\delta_{ij}+2A(1-A)(p_\perp+\tfrac{1}{2}q_\perp)_i(p_\perp-\tfrac{1}{2}q_\perp)_j$$
$$-\tfrac{1}{2}A(1-A)k^2\delta_{ij}][(\mathbf{p}_\perp+\tfrac{1}{2}\mathbf{q}_\perp)^2+m^2-A(1-A)k^2]^{-1}$$
$$\times[(\mathbf{p}_\perp-\tfrac{1}{2}\mathbf{q}_\perp)^2+m^2-A(1-A)k^2]^{-1}\}. \quad (4.7)$$

Note that (4.7) makes sense only if $k^2<4m^2$, i.e., when the virtual photon is stable against decaying into an electron-positron pair. In view of Fig. 1, we shall assume throughout that k is spacelike:

$$k^2\leq 0. \quad (4.8)$$

The introduction of a Feynman parameter x reduces (4.7) to

$$g^\gamma(\mathbf{q}_\perp)=-\tfrac{1}{2}\pi^{-2}e^4\int_0^1 dA\int_0^1 dx\{\tfrac{1}{2}A(1-A)\delta_{ij}|k^2|$$
$$\times[m^2+A(1-A)|k^2|]^{-1}-[\tfrac{1}{4}\delta_{ij}\mathbf{q}_\perp^2$$
$$+\tfrac{1}{2}A(1-A)\delta_{ij}|k^2|-2A(1-A)x(1-x)q_{\perp i}q_{\perp j}]$$
$$\times[x(1-x)\mathbf{q}_\perp^2+m^2+A(1-A)|k^2|]^{-1}$$
$$+A(1-A)\delta_{ij}\ln[x(1-x)\mathbf{q}_\perp^2+m^2+A(1-A)|k^2|]/$$
$$[m^2+A(1-A)|k^2|]\}. \quad (4.9)$$

B. Impact Factor for Large $|k^2|$

As a first step, we want to study $g^\gamma(\mathbf{q}_\perp)$, as given by (4.9), for large $|k^2|$ but fixed $\mathbf{q}_\perp$. For this purpose it is convenient to write

$$g^\gamma(\mathbf{q}_\perp)=-\tfrac{1}{2}\pi^{-2}e^4[\delta_{ij}I_1+(q_{\perp i}q_{\perp j}-\tfrac{1}{2}\mathbf{q}_\perp^2\delta_{ij})I_2], \quad (4.10)$$

where

$$I_1=\int_0^1 dA\int_0^1 dx\{-\tfrac{1}{2}m^2[m^2+A(1-A)|k^2|]^{-1}$$
$$-[\mathbf{q}_\perp^2(\tfrac{1}{2}-x+x^2)(\tfrac{1}{2}-A+A^2)-\tfrac{1}{2}m^2]$$
$$\times[x(1-x)\mathbf{q}_\perp^2+m^2+A(1-A)|k^2|]^{-1}\} \quad (4.11)$$

and

$$I_2=\int_0^1 dA\int_0^1 dx\, 2A(1-A)x(1-x)$$
$$\times[x(1-x)\mathbf{q}_\perp^2+m^2+A(1-A)|k^2|]^{-1}. \quad (4.12)$$

When $|k^2|\to\infty$ with $\mathbf{q}_\perp$ fixed, we can neglect $\mathbf{q}_\perp$ altogether in (4.12). Thus, in this limit,

$$I_2\sim\int_0^1 dA\int_0^1 dx\, 2x(1-x)|k^2|^{-1}=\tfrac{1}{3}|k^2|^{-1}. \quad (4.13)$$

The behavior of I_1 is much more complicated. Let $\bar{I}_1(\zeta)$ be the Mellin transform of I_1:

$$\bar{I}_1(\zeta)=\int_0^\infty d|k^2|\,(|k^2|/m^2)^{-\zeta}I_1, \quad (4.14)$$

then, for ζ small and positive,

$$\bar{I}_1(\zeta)=m^{2\zeta}\pi\csc(\pi\zeta)\int_0^1 dA\int_0^1 dx\{-\tfrac{1}{2}m^{2(1-\zeta)}$$
$$\times[A(1-A)]^{-1+\zeta}-[\mathbf{q}_\perp^2(\tfrac{1}{2}-x+x^2)(\tfrac{1}{2}-A+A^2)-\tfrac{1}{2}m^2][m^2+x(1-x)\mathbf{q}_\perp^2]^{-\zeta}[A(1-A)]^{-1+\zeta}\}$$
$$=\pi\csc(\pi\zeta)[\Gamma(\zeta)]^2[\Gamma(2\zeta)]^{-1}\int_0^1 dx\{-\tfrac{1}{2}m^2-[\tfrac{1}{2}\mathbf{q}_\perp^2(1+\zeta)(1+2\zeta)^{-1}(\tfrac{1}{2}-x+x^2)-\tfrac{1}{2}m^2][1+x(1-x)\mathbf{q}_\perp^2/m^2]^{-\zeta}\}$$
$$\sim 2\zeta^{-2}\left\{-\tfrac{1}{6}\mathbf{q}_\perp^2(1-\zeta)+\zeta\int_0^1 dx[\tfrac{1}{2}\mathbf{q}_\perp^2(\tfrac{1}{2}-x+x^2)-\tfrac{1}{2}m^2]\ln[1+x(1-x)\mathbf{q}_\perp^2/m^2]\right\}$$
$$=2\zeta^{-2}\{-\tfrac{1}{6}\mathbf{q}_\perp^2-(7/36)\zeta\mathbf{q}_\perp^2+\tfrac{2}{3}\zeta m^2+\tfrac{2}{3}\zeta(\mathbf{q}_\perp^2-2m^2)(\tfrac{1}{4}+m^2/\mathbf{q}_\perp^2)^{1/2}\ln[\tfrac{1}{2}(\mathbf{q}_\perp^2/m^2)^{1/2}+(1+\tfrac{1}{4}\mathbf{q}_\perp^2/m^2)^{1/2}]\}. \quad (4.15)$$

It follows immediately from (4.15) and (4.14) that, as $|k^2|\to\infty$ with fixed $\mathbf{q}_\perp$,

$$I_1\sim 2|k^2|^{-1}\{-\tfrac{1}{6}\mathbf{q}_\perp^2\ln(|k^2|/m^2)-(7/36)\mathbf{q}_\perp^2+\tfrac{2}{3}m^2$$
$$+\tfrac{2}{3}(\mathbf{q}_\perp^2-2m^2)(\tfrac{1}{4}+m^2/\mathbf{q}_\perp^2)^{1/2}$$
$$\times\ln[\tfrac{1}{2}(\mathbf{q}_\perp^2/m^2)^{1/2}+(1+\tfrac{1}{4}\mathbf{q}_\perp^2/m^2)^{1/2}]\}. \quad (4.16)$$

C. Matrix Element for Large $|k^2|$

We substitute the results of Sec. B for the photon impact factor into (4.6). For large $|k^2|$ but fixed nonzero values of m and λ, we ask what the important region is for the variable $\mathbf{q}_\perp$. A moment's reflection indicates that the answer is

$$m^2\ll\mathbf{q}_\perp^2\ll|k^2|. \quad (4.17)$$

By rotational symmetry, the I_2 of (4.10) does not contribute. And it is sufficient to use the I_1 of (4.16). Moreover, the right-hand side of (4.16) can be simplified in the region (4.17). When (4.17) is satisfied,

$$I_1\sim-\tfrac{1}{3}|k^2|^{-1}\mathbf{q}_\perp^2[\ln(|k^2|/\mathbf{q}_\perp^2)+7/6]. \quad (4.18)$$

It is interesting to note that the fermion mass m does not appear in (4.18).

It only remains to substitute (4.18) into (4.6) to get that, for large $|k^2|$ with fixed m and λ,

$$\lim_{\omega\to\infty}(-i\omega^{-1}\mathfrak{M}_0^{(D)})$$
$$=(2\pi)^{-2}e^2Z^2\int d\mathbf{q}_\perp(\mathbf{q}_\perp^2+\lambda^2)^{-2}g^\gamma(\mathbf{q}_\perp)$$
$$=(2\pi)^{-3}e^6Z^2\int_0^{|k^2|}d\mathbf{q}_\perp^2(\mathbf{q}_\perp^2+\lambda^2)^{-2}\{\tfrac{1}{3}|k^2|^{-1}\mathbf{q}_\perp^2$$
$$\times[\ln(|k^2|/\mathbf{q}_\perp^2)+7/6]\}+O(|k^2|^{-1})$$
$$=\tfrac{1}{6}(2\pi)^{-3}e^6Z^2|k^2|^{-1}\{[\ln(|k^2|/\lambda^2)]^2$$
$$+\tfrac{1}{3}\ln(|k^2|/\lambda^2)+O(1)\}. \quad (4.19)$$

This is the desired answer. Of course, the absence of m in (4.18) implies the absence of m in (4.19).

D. Remarks

(i) The terms of order 1, not explicitly given in (4.19), are rather complicated. The present procedure is not powerful enough to yield these terms; they are derived in Appendix B.

(ii) The logarithm-squared term in (4.19) comes from the region $\mathbf{p}_\perp^2\ll|k^2|$ and $\mathbf{q}_\perp^2\ll|k^2|$. If the fermion has a rapidly decreasing electromagnetic form factor, this logarithm-squared term disappears. Whether the logarithmic term also disappears is difficult to ascertain,

but we think it is unlikely. The meaning of logarithmic terms is unclear to the authors.

(iii) If we ignore the logarithmic terms, then we see, both from the denominators in (4.7) and also from (4.6) or (4.19), that the important scale for the transverse momentum transfers $\mathbf{p}_\perp$ and $\mathbf{q}_\perp$ is $|k^2|^{1/2}$. This verifies our conjecture that the difficulty in making large transverse momentum transfers at high energies is much less when $|k^2|$ is larger.

(iv) Equation (4.19) implies in particular that the total cross section for the scattering of a virtual photon of given k^2 on a static Coulomb field approaches a constant at infinite energy.

5. DELBRÜCK SCATTERING OFF THE MASS SHELL—LONGITUDINAL PHOTON

In Sec. 4, the photon was assumed to be transverse. We repeat here all the considerations for a longitudinal photon.

With $k^2<0$, the four-vector k can be chosen to be

$$k=(\omega,\ (\omega^2+|k^2|)^{1/2},\ 0,\ 0), \tag{5.1}$$

while the polarization vector for longitudinal photon is

$$\epsilon_L=((1+\omega^2/|k^2|)^{1/2},\ \omega|k^2|^{-1/2},\ 0,\ 0). \tag{5.2}$$

By (5.1) and the conservation of current, the polarization vector (5.2) can be replaced by

$$\epsilon_L'=\epsilon_L-\omega^{-1}(1+\omega^2/|k^2|)^{1/2}k = (0,\ -\omega^{-1}|k^2|^{1/2},\ 0,\ 0). \tag{5.3}$$

With this polarization vector, we define, for $i=1,\ 2$,

$$R_{iL}=\epsilon_L'R_i\epsilon_L',$$

$$g_L{}^\gamma(\mathbf{q}_\perp)=\lim_{\omega\to\infty}(2\pi)^{-1}\int_{-\infty}^{\infty}dq_3\frac{R_{1L}+R_{2L}}{\omega},$$

and

$$\mathfrak{M}_{0L}{}^{(D)}=\epsilon_L'\mathfrak{M}_0{}^{(D)}\epsilon_L' \sim i\omega(2\pi)^{-2}e^2Z^2\int d\mathbf{q}_\perp(\mathbf{q}_\perp{}^2+\lambda^2)^{-2}g_L{}^\gamma(\mathbf{q}_\perp) \tag{5.4}$$

for large ω. In (5.4), R_1 and R_2 are given by (4.4) and (4.5), respectively.

Because, as $\omega\to\infty$,

$$\epsilon_L'k\sim-|k^2|^{1/2}$$

and

$$\epsilon_L'p\sim A|k^2|^{1/2}\quad\text{or}\quad(A-\tfrac{1}{2})|k^2|^{1/2} \tag{5.5}$$

in connection with (4.4) and (4.5), respectively, we have explicitly

$$R_{1L}\sim 2(2\pi)^{-4}e^4\int d^4p[(k+p)^2-m^2]^{-1}(p^2-m^2)^{-2} \times[(p+q)^2-m^2]^{-1}[-32A^3(1-A)|k^2|\omega^2] \tag{5.6}$$

and

$$R_{2L}\sim(2\pi)^{-4}e^4\int d^4p[(\tfrac{1}{2}k-p-\tfrac{1}{2}q)^2-m^2]^{-1} \times[(\tfrac{1}{2}k-p+\tfrac{1}{2}q)^2-m^2]^{-1}[(-\tfrac{1}{2}k-p+\tfrac{1}{2}q)^2-m^2]^{-1} \times[(-\tfrac{1}{2}k-p-\tfrac{1}{2}q)^2-m^2]^{-1} \times[32A^2(1-A)^2|k^2|\omega^2]. \tag{5.7}$$

Accordingly, in analogy with (4.7) and (4.9), the longitudinal-photon impact factor is given by

$$\begin{aligned}g_L{}^\gamma(\mathbf{q}_\perp)&=\pi^{-3}e^4|k^2|\int d\mathbf{p}_\perp\int_0^1 dA\ A^2(1-A)^2\\ &\times\{[\mathbf{p}_\perp{}^2+m^2+A(1-A)|k^2|]^{-2}\\ &-[(\mathbf{p}_\perp+\tfrac{1}{2}\mathbf{q}_\perp)^2+m^2+A(1-A)|k^2|]^{-1}\\ &\times[(\mathbf{p}_\perp-\tfrac{1}{2}\mathbf{q}_\perp)^2+m^2+A(1-A)|k^2|]^{-1}\}\\ &=\pi^{-2}e^4|k^2|\int_0^1 dA\int_0^1 dx\ A^2(1-A)^2\\ &\times\{[m^2+A(1-A)|k^2|]^{-1}\\ &-[x(1-x)\mathbf{q}_\perp{}^2+m^2+A(1-A)|k^2|]^{-1}\}\\ &=-\pi^{-2}e^4\int_0^1 dA\int_0^1 dx\ A(1-A)\\ &\times\{m^2[m^2+A(1-A)|k^2|]^{-1}\\ &-[x(1-x)\mathbf{q}_\perp{}^2+m^2][x(1-x)\mathbf{q}_\perp{}^2+m^2\\ &+A(1-A)|k^2|]^{-1}\}.\end{aligned} \tag{5.8}$$

For large $|k^2|$ but fixed $\mathbf{q}_\perp$, we can replace both denominators by $A(1-A)|k^2|$. Thus, in this limit,

$$g_L{}^\gamma(\mathbf{q}_\perp)\sim\tfrac{1}{6}\pi^{-2}e^4|k^2|^{-1}\mathbf{q}_\perp{}^2. \tag{5.9}$$

Unlike (4.16), there is no logarithmic factor.

Finally, (5.9) may be substituted into (5.4) to yield, for large $|k^2|$ with fixed nonzero values of m and λ,

$$\begin{aligned}\lim_{\omega\to\infty}(-i\omega^{-1}\mathfrak{M}_{0L}{}^{(D)})&=(2\pi)^{-2}e^2Z^2\int d\mathbf{q}_\perp(\mathbf{q}_\perp{}^2+\lambda^2)^{-2}g_L{}^\gamma(\mathbf{q}_\perp)\\ &=\tfrac{1}{3}(2\pi)^{-3}e^6Z^2\int_0^{|k^2|}d\mathbf{q}_\perp{}^2|k^2|^{-1}\mathbf{q}_\perp{}^2(\mathbf{q}_\perp{}^2+\lambda^2)^{-2}\\ &\quad+O(|k^2|^{-1})\\ &=\tfrac{1}{3}(2\pi)^{-3}e^6Z^2|k^2|^{-1}[\ln(|k^2|/\lambda^2)+O(1)].\end{aligned} \tag{5.10}$$

This is the desired answer.

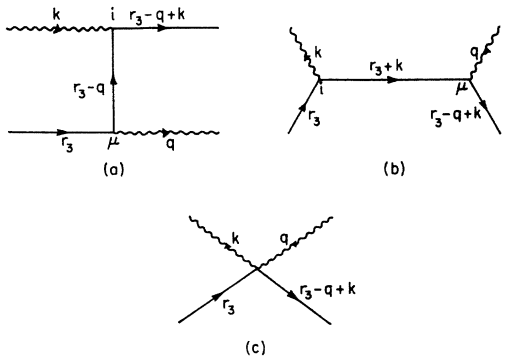

FIG. 4. Compton scattering of a virtual photon by a scalar meson.

The terms of order 1 are found in Appendix C to be $-\frac{4}{3}$. Note that remark (iii) of Sec. 4D also applies here.

6. COMPTON SCATTERING OFF SCALAR MESONS

A. Motivation

In Secs. 4 and 5, we have shown that the Delbrück scattering amplitude goes down as $-k^2$ increases, and diffraction scattering becomes less important. We therefore expect other competing processes to take on more prominent roles, and as a consequence the production amplitude is less peaked. In order to substantiate these statements, we shall, in this section and Sec. 7, attempt to investigate (1) the order of magnitude of some of the competing processes, (2) the qualitative behavior of the differential cross sections for such processes.

The simplest process is the Compton scattering process, where the virtual photon is absorbed and a real photon is emitted. Although at $k^2=0$, this amplitude is smaller than the Delbrück amplitude by a factor of s at high energies, they will be shown to be of the same order of magnitude when $-k^2$ is comparable to s. It is therefore instructive to investigate Compton scattering in some detail.

B. Calculations

We shall first study the academic case in which the proton is treated as a scalar meson. The Feynman diagrams considered are illustrated in Fig. 4. The corresponding amplitude is given by

$$\mathfrak{M}_{\mu i}=-2e^2\{(r_3-q)_i(2r_3-q)_\mu/[(r_3-q)^2-m_p^2] +r_{3i}(2r_3+2k-q)_\mu/(s-m_p^2)-g_{i\mu}\}, \quad (6.1)$$

where the condition $k_i=0$ has been used. To simplify the calculations on the differential cross section, we shall obtain only the sum over the polarization of the emitted photon. From (6.1), we have

$$\begin{aligned}\sum_\mu \mathfrak{M}_{\mu i}\mathfrak{M}_{\mu j}^*=4e^4\{&(r_3-q)_i(r_3-q)_j(2r_3-q)^2\\ &\times[(r_3-q)^2-m_p^2]^{-2}+r_{3i}r_{3j}(2r_3+2k-q)^2(s-m_p^2)^{-2}\\ &+g_{ij}-[(r_3-q)_i(2r_3-q)_j+(2r_3-q)_i(r_3-q)_j]\\ &\times[(r_3-q)^2-m_p^2]^{-1}-[r_{3i}(2r_3-q)_j+(2r_3-q)_ir_{3j}]\\ &\times(s-m_p^2)^{-1}+[(r_3-q)_ir_{3j}+r_{3i}(r_3-q)_j][(2r_3-q)\\ &\times(2r_3+2k-q)](s-m_p^2)^{-1}[(r_3-q)^2-m_p^2]^{-1}\}. \quad (6.2)\end{aligned}$$

Note that $\mathfrak{M}_{\mu j}$ is real as none of the denominators in (6.1) vanish.

The calculations will be carried out in the c.m. system. In this system, we denote

$$\begin{aligned}k\sim&(aW+[\lambda^2+\tfrac{1}{2}(1-a)m_p^2]\\ &\times(1+a)^{-1}W^{-1}, W, 0, 0),\\ r_3\sim&(W+\tfrac{1}{2}m_p^2W^{-1}, -W, 0, 0),\\ q\sim&(\tfrac{1}{2}(1+a)W+\lambda^2(1+a)^{-1}W^{-1}, -\tfrac{1}{2}(1+a)W\\ &\times\cos\Theta, -\tfrac{1}{2}(1+a)W\sin\Theta, 0),\end{aligned}$$

$$r_3+k-q\sim(\tfrac{1}{2}(1+a)W+\frac{m_p^2}{(1+a)W}, \tfrac{1}{2}(1+a)W \times\cos\Theta, \tfrac{1}{2}(1+a)W\sin\Theta, 0), \quad (6.3)$$

where λ is the introduced mass of the emitted photon. We are considering the high energy limit $W\to\infty$ and terms of the order of W^{-2} in (6.3) have been discarded.

From (6.3), we obtain

$$(r_3-q)^2-m_p^2=-[(1+a)W^2(1-\cos\Theta)+\tfrac{1}{2}(1+a)m_p^2 +\lambda^2(1-a)(1+a)^{-1}], \quad (6.4)$$

which is of the order of W^2 except when the momenta of the proton and the emitted photon are parallel so that $\Theta=0$. And at $\Theta=0$, the right side of (6.4) is finite as $W\to\infty$.

As a result, $\mathfrak{M}_{\mu i}$ as given by (6.1) is peaked around $\Theta=0$. Because of the first term in the right side of (6.1), it is of the order of W^2 at $\Theta=0$, and is of the order of unity when $\Theta\neq 0$. However, this peak in reality is damped when $-k^2$ becomes large. This is because at $\Theta\doteq 0$, the internal proton in Fig. 4(a) is almost on the mass shell, and the upper vertex gives an additional proton form factor which goes down very rapidly as k^2 becomes large. With the proton form factor not taken into consideration, one may expect that $\sum_\mu \mathfrak{M}_{\mu i}\mathfrak{M}_{\mu j}^*$ is of the order of W^4 at $\Theta=0$. This is not the case. Substituting

$$\begin{aligned}&(2r_3-q)^2\\ &=2(r_3-q)^2+2r_3^2-q^2=2[(r_3-q)^2-m_p^2]+4m_p^2-\lambda^2,\\ &(2r_3+2k-q)^2\\ &=2(r_3+k)^2+2(r_3+k-q)^2-q^2=2(s-m_p^2)+4m_p^2-\lambda^2,\\ &(2r_3-q)(2r_3+2k-q)\\ &=[(r_3-q)^2-m_p^2]+(s-m_p^2)+4m_p^2-\lambda^2-2k^2,\end{aligned}$$

into (6.2), we get

$$\sum_\mu \mathfrak{M}_{\mu i}\mathfrak{M}_{\mu j}^* \sim 4e^4\{(r_3-q)_i(r_3-q)_j(4m_p^2-\lambda^2) \times[(r_3-q)^2-m_p^2]^{-2}+g_{ij} -2k^2[(r_3-q)_i r_{3j}+r_{3i}(r_3-q)_j] \times[(r_3-q)^2-m_p^2]^{-1}(s-m_p^2)]^{-1}\}, \quad (6.5)$$

where two of the terms, $4e^2 r_{3i}r_{3j}(4m_p^2-\lambda^2)(s-m_p^2)^{-2}$ and

$$4e^2[(r_3-q)_i r_{3j}+r_{3i}(r_3-q)_j](4m_p^2-\lambda^2) \times(s-m_p^2)^{-1}[(r_3-q)^2-m_p^2]^{-1},$$

have been discarded.

We shall evaluate the right side of (6.5) for various polarizations. The polarization vector of the virtual photon may be either transverse or longitudinal. We list the three independent polarization vectors as follows:

transverse: (0,0,0,1), (0,0,1,0);

longitudinal: $(1,a,0,0)/(1-a^2)^{1/2}$.

The differential cross section is given by

$$d\sigma/d\Omega = -(16\pi^2 aW^2)^{-1}\sum_\mu \mathfrak{M}_{\mu i}\mathfrak{M}_{\mu j}^*|_{i=j}.$$

Now, when the virtual photon has the polarization (0,0,0,1) or (0,0,1,0), r_{3i} vanishes, and q_i vanishes for (0,0,0,1) and is proportional to $\sin\Theta$ for (0,0,1,0). In either case, the first and the third term in the right side of (6.5) do not contribute. Thus, for transverse virtual photon we have

$$d\sigma_T/d\Omega \sim (4\pi^2 aW^2)^{-1}e^4, \quad W\to\infty \quad (6.6)$$

and

$$\sigma_T \sim (\pi aW^2)^{-1}e^4, \quad W\to\infty. \quad (6.7)$$

Note that the differential cross section in (6.6) is isotropic.

If the polarization of the virtual photon is longitudinal, we have

$$r_{3i}\sim(1+a)^{1/2}(1-a)^{-1/2}W, \quad (6.8)$$

$$q_i\sim(1+a)^{1/2}(1-a)^{-1/2}W\tfrac{1}{2}(1+a\cos\Theta). \quad (6.9)$$

Thus, in the limit $W\to\infty$, we have, for longitudinal virtual photons,

$$d\sigma_L/d\Omega \sim (4\pi^2 aW^2)^{-1}e^4\{-\tfrac{1}{4}(1+a)(1-a)^{-1}(1-a\cos\Theta)^2 \times(4m_p^2-\lambda^2)W^2[(1+a)W^2(1-\cos\Theta)+\tfrac{1}{2}(1+a)m_p^2 +\lambda^2(1-a)(1+a)^{-1}]^{-2}-1+2W^2(1-a\cos\Theta) \times[(1+a)W^2(1-\cos\Theta)+\tfrac{1}{2}(1+a)m_p^2 +\lambda^2(1-a)(1+a)^{-1}]\} \quad (6.10)$$

and

$$\sigma_L\sim(\pi aW^2)^{-1}e^4(1-a)(1+a)^{-1}\{-1+\ln W^2 -\ln[\tfrac{1}{4}m_p^2+\tfrac{1}{2}\lambda^2(1-a)(1+a)^{-2}]-\tfrac{1}{4}(4m_p^2-\lambda^2) \times[m_p^2+2\lambda^2(1-a)(1+a)^{-2}]^{-1}\}. \quad (6.11)$$

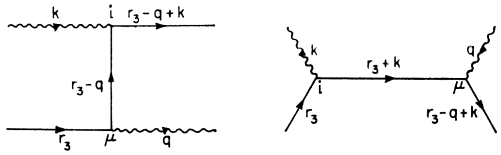

FIG. 5. Compton scattering of a virtual photon by a fermion.

C. Remarks

(i) The differential cross sections for Compton scattering as given by (6.6) and (6.10) are of the same order of magnitude as those for Delbrück scattering when $-k^2$ and s are comparable. This is consistent with our conjecture that diffraction scattering is no more dominant when $-k^2$ and s are comparable.

(ii) The differential cross section given by (6.6) for transverse photons is isotropic, while that given by (6.10) is peaked around $\Theta=0$. This peak, however, is expected to be damped by the presence of the proton form factor. This is consistent with our conjecture that the scattering spreads out as $-k^2$ increases.

(iii) The integrated cross section for transverse photons given by (6.7) is proportional to W^{-2}, while that for longitudinal photons given by (6.11) has a term proportional to $W^{-2}\ln W^2$. The factor $\ln W^2$ is expected to disappear if the proton form factor is taken into account. Therefore, neither of the polarizations is favored over the other.

7. COMPTON SCATTERING OFF FERMIONS

Continuing our investigation on competing processes, we shall now study the Compton scattering of a virtual photon on a proton treated as a fermion.

The Feynman diagrams considered are illustrated in Fig. 5. The corresponding amplitude is given by

$$\mathfrak{M}_{\mu i} = -e^2\{\gamma_i(r_3-q+m_p)\gamma_\mu[(r_3-q)^2-m_p^2]^{-1} +\gamma_\mu(r_3+k+m_p)\gamma_i(s-m_p^2)^{-1}\}. \quad (7.1)$$

From (7.1), we obtain

$$\tfrac{1}{2}\sum_{\text{electron spins}}\sum_\mu \mathfrak{M}_{\mu i}\mathfrak{M}_{\mu j}^* = (8m^2)^{-1}e^4\{T_{11}[(r_3-q)^2-m_p^2]^{-2}+T_{22}(s-m_p^2)^{-2} +(T_{12}+T_{21})[(r_3-q)^2-m_p^2]^{-1}(s-m_p^2)^{-1}\}, \quad (7.2)$$

where

$$T_{11}=\mathrm{Tr}[\gamma_i(r_3-q+m_p)\gamma_\mu(r_3+m_p)\gamma_\mu(r_3-q+m_p) \times\gamma_j(r_3-q+k+m_p)], \quad (7.3)$$

$$T_{12}=\mathrm{Tr}[\gamma_i(r_3-q+m_p)\gamma_\mu(r_3+m_p)\gamma_j(r_3+k+m_p) \times\gamma_\mu(r_3-q+k+m_p)], \quad (7.4)$$

$$T_{21}=T_{12}(i\leftrightarrow j), \quad (7.5)$$

$$T_{22}=\mathrm{Tr}[\gamma_\mu(r_3+k+m_p)\gamma_i(r_3+m_p)\gamma_j(r_3+k+m_p) \times\gamma_\mu(r_3-q+k+m_p)]. \quad (7.6)$$

Only the following terms are important when $i=j$:

$$T_{11}=4(2m_p^2+\lambda^2)[4(r_3-q)_i(r_3-q)_j+k^2g_{ij}] +4[(r_3-q)^2-m_p^2] \times[4(r_3-q)_iq_j-g_{ij}(s-m_p^2)], \quad (7.7)$$

$$T_{22}=4(2m_p^2+\lambda^2)[4r_{3i}r_{3j}-g_{ij}(s-m_p^2-\lambda^2)] +8(s-m_p^2)[-2q_jr_{3i}+g_{ij}(r_3q+m_p^2)], \quad (7.8)$$

and

$$T_{12}\sim 4k^2\{[(r_3-q)^2-k^2]g_{ij}-2r_{3i}r_{3j}-2(r_3-q)_i(r_3-q)_j\} +4s[2q_i(q-r_3)_j+k^2g_{ij}]+8(r_3-q)^2r_{3i}q_j. \quad (7.9)$$

The differential cross section is given by

$$d\sigma/d\Omega=-(64\pi^2aW^2)^{-1}m^2\tfrac{1}{2}\sum_{\text{electron spins}}\sum_{\mu}\mathfrak{M}_{\mu i}\mathfrak{M}_{\mu j}^*.$$

Substituting (7.7)–(7.9) into (7.2), we get, after some algebraic manipulations:

$$\frac{d\sigma}{d\Omega}\sim\frac{\alpha^2}{8aW^2}\left(\frac{(2m_p^2+\lambda^2)[4(r_3-q)_i(r_3-q)_j-W^2(1-a^2)g_{ij}]}{[(1+a)W^2(1-\cos\Theta)+\frac{1}{2}(1+a)m_p^2+\lambda^2(1-a)/(1+a)]^2} +\frac{-4[(1-a)/(1+a)][r_{3i}r_{3j}+(r_3-q)_i(r_3-q)_j]+g_{ij}W^2(4+a^2-2a\cos\Theta+\cos^2\Theta)}{(1+a)W^2(1-\cos\Theta)+\frac{1}{2}(1+a)m_p^2+\lambda^2(1-a)/(1+a)}\right). \quad (7.10)$$

When the polarization of the virtual photon is (0,0,0,1), we have

$$\frac{d\sigma_{T1}}{d\Omega}\sim\frac{\alpha^2}{8aW^2}\left(\frac{-(2m_p^2+\lambda^2)W^2(1-a^2)}{[(1+a)W^2(1-\cos\Theta)+\frac{1}{2}(1+a)m_p^2+\lambda^2(1-a)/(1+a)]^2} +\frac{W^2(4+a^2-2a\cos\Theta+\cos^2\Theta)}{(1+a)W^2(1-\cos\Theta)+\frac{1}{2}(1+a)m_p^2+\lambda^2(1-a)/(1+a)}\right) \quad (7.11)$$

and

$$\sigma_{T1}\sim\frac{\pi\alpha^2}{4aW^2}\left(\frac{-(2m_p^2+\lambda^2)(1-a)}{\frac{1}{2}(1+a)m_p^2+\lambda^2(1-a)/(1+a)}+\frac{5-2a+a^2}{1+a}\ln\frac{W^2}{\frac{1}{4}m_p^2+\frac{1}{2}\lambda^2(1-a)/(1+a)^2}+2\frac{2a-1}{1+a}\right). \quad (7.12)$$

When the polarization of the virtual photon is (0,0,1,0), we have

$$\frac{d\sigma_{T2}}{d\Omega}\sim\frac{d\sigma_{T1}}{d\Omega}+\frac{\alpha^2}{8a}\frac{(1-a^2)\sin^2\Theta}{(1+a)W^2(1-\cos\Theta)+\frac{1}{2}(1+a)m_p^2+\lambda^2(1-a)/(1+a)} \quad (7.13)$$

and

$$\sigma_{T2}\sim\sigma_{T1}+\alpha^2\pi(2aW^2)^{-1}(1-a). \quad (7.14)$$

When the polarization of the virtual photon is longitudinal, we have

$$d\sigma_L/d\Omega\sim\alpha^2(8aW^2)^{-1}(1-a)(1+\cos\Theta), \quad (7.15)$$

and

$$\sigma_L\sim\alpha^2\pi(2aW^2)^{-1}(1-a)\sim\sigma_{T2}-\sigma_{T1}. \quad (7.16)$$

We wish to make the following remarks:

(i) In the above calculations, we have discarded all terms in $d\sigma/d\Omega$ which, in the limit $W\to\infty$, are negligible both for $\Theta\neq 0$ (compared with W^{-2}) and at $\Theta=0$ (compared with unity). Thus, terms of the order of $W^2m_p^2$ in T_{22} and T_{12} are neglected.

(ii) The differential cross section for longitudinal virtual photons, as given by (7.15), has no sharp peak, while those for transverse virtual photons, as given by (7.11) and (7.13), are sharply peaked around $\Theta=0$. This is just the opposite of the scalar case treated in Sec. 6. As before, we expect this peak to be flattened by the proton form factor. The disappearance of $\ln W^2$ from the expressions (7.12) and (7.14) is also anticipated when the proton form factor is taken into account. However, if high-order diagrams are calculated, the proton form factor is not expected to be able to suppress *all* logarithmic functions.

8. DISCUSSIONS

We emphasize from both the present considerations and the previous calculations on quantum electrodynamics[6] that numerators in the integral expression for matrix elements play an extremely important role. For example, as most clearly seen in III, the dominating contribution comes from the vicinity of the zero of one of the Feynman parameters (α_1 in the notation there) when there is no numerator, but this is no longer true with the numerator due to the fermion spin. Accordingly model calculations with spin-zero particles only are presumably not relevant to inelastic electron scattering.

We have seen in the last few sections that logarithmic factors like $\ln(|k^2|/\lambda^2)$ appear very frequently. For energies available from existing electron accelerators, this logarithmic factor is never large. If we neglect such factors, then the only important scale for transverse momentum transfers is $|k^2|^{1/2}$, when $|k^2|$ is large. In

other words, for large $|k^2|$, the hadron masses are not important. Thus, by dimensional arguments, various quantities are approximately of the form of a product of a function of $\nu|k^2|^{-1}$ with an appropriate power of ν. This includes, as a special case, the universal representation of the deep inelastic scattering reported by Panofsky[11]:

$$\nu W_2(-k^2, \nu) = \text{function of } (\nu|k^2|^{-1}). \quad (8.1)$$

Moreover, if the results of Secs. 4 and 5 are taken seriously, this function of $\nu|k^2|^{-1}$ approaches a constant for large values of the argument.

If the logarithmic factors are not discarded, the dimensional argument no longer holds,[12] and (8.1) is not true. Instead, we have only the following weaker statement: For fixed $\nu|k^2|^{-1}$, $\nu W_2(-k^2, \nu)$ is a slowly varying function of ν. In this connection, it may be interesting to note from Panofsky[11] that in the reported data $|k^2|$ only goes up to 2.3 $(\text{BeV}/c)^2$. If λ is taken to be the mass of ρ meson, $\ln(|k^2|/\lambda^2)$ is only about 1.4. Thus, from the present point of view, the experimental evidence from (8.1) is still weak. Convincing evidence for or against (8.1) must come from inelastic electron scattering at larger angles θ.[13]

ACKNOWLEDGMENTS

We are greatly indebted to Professor C. N. Yang for numerous discussions on high-energy processes. We also wish to thank Dr. Luke W. Mo for an informative conversation of SLAC experiments.

APPENDIX A

Let us recall Fermi's picture of high-energy scattering.[7] In this picture, two particles with large energies collide and a small volume surrounding the two particles is suddenly heated up. Very rapidly statistical equilibrium is achieved and the energy is distributed among the various degrees of freedom according to statistical laws and the particles will fly out in all directions. The Fermi model is now well explored.[8]

Fermi's idea, however, cannot account for diffraction scattering in any way. In fact, we now know that, in quantum electrodynamics, the high-energy two-body elastic scattering near the forward direction proceeds through an entirely different manner.[6] Even when large-angle scattering is considered, it is not known what percentage of the collisions should be considered statistical and whether the tail of the diffraction peak would hide the effects under consideration.

From our point of view, the region $-k^2 \to \infty$, $-k^2/s$ finite, offers the best chance that the statistical model of Fermi may become reality. The photon must be absorbed in a very small region inside the proton, and this region is suddenly heated up and a very hot center is formed. Many particles are created, collide, and fly out in all directions. This process is therefore much closer to Fermi's visualization than the nucleon-nucleon scattering process for which Fermi's model was originally conceived. The absence of a diffraction peak in this limit also offers a more unambiguous test of the statistical part of the scattering. Even in this extreme limit, the validity of Fermi's model is by no means certain. For example, we know of no reason why anything like statistical equilibrium should be attained in high-energy scattering. Experimental tests would therefore be interesting.

APPENDIX B

In this appendix, we give an alternative derivation of (4.19). The substitution of (4.7) into (4.6) gives, when $\omega \to \infty$,

$$\mathfrak{M}_0^{(D)} \sim (2\pi)^{-3} i\omega e^6 Z^2 \delta_{ij} M(k^2), \quad (B1)$$

where

$$M(k^2) = -\pi^{-2} \int d\mathbf{q}_\perp \, (\mathbf{q}_\perp^2+\lambda^2)^{-2} \int d\mathbf{p}_\perp \int_0^1 dA \{A(1-A)(\mathbf{p}_\perp^2+\tfrac{1}{2}|k^2|)[\mathbf{p}_\perp^2+m^2+A(1-A)|k^2|]^{-2}$$
$$-[\tfrac{1}{4}\mathbf{q}_\perp^2+A(1-A)(\mathbf{p}_\perp^2-\tfrac{1}{4}\mathbf{q}_\perp^2)+\tfrac{1}{2}A(1-A)|k^2|][(\mathbf{p}_\perp+\tfrac{1}{2}\mathbf{q}_\perp)^2+m^2+A(1-A)|k^2|]^{-1}$$
$$\times[(\mathbf{p}_\perp-\tfrac{1}{2}\mathbf{q}_\perp)^2+m^2+A(1-A)|k^2|]^{-1}\}. \quad (B2)$$

Introduction of the Feynman parameter x together with an integration by parts with respect to $\mathbf{q}_\perp^2$ reduces (B2) to

$$M(k^2) = \int_0^\infty d\mathbf{q}_\perp^2 \, (\mathbf{q}_\perp^2+\lambda^2)^{-1} \int_0^1 dx \int_0^1 dA[x(1-x)\mathbf{q}_\perp^2+m^2+A(1-A)|k^2|]^{-2}$$
$$\times\{A(1-A)(\tfrac{1}{2}-A+A^2)(\tfrac{1}{2}-x+x^2)|k^2|+[\tfrac{1}{4}-\tfrac{1}{2}A(1-A)+x(1-x)A(1-A)]m^2\}. \quad (B3)$$

[11] W. K. H. Panofsky, in *Proceedings of the Fourteenth International Conference on High-Energy Physics Vienna* (CERN, Geneva, 1968), p. 36.
[12] H. Cheng and T. T. Wu, Phys. Rev. Letters 22, 1409 (1969).
[13] We understand that experiment at $\theta = 18°$ has already been carried out at SLAC.

Similarly to (4.14), we take the Mellin transform of (B3)

$$\bar{M}(\zeta)=\int_0^\infty d|k^2|\ (|k^2|/m^2)^{-\zeta}M(k^2)$$

$$=m^{2\zeta}\pi\csc(\pi\zeta)\int_0^\infty d\mathbf{q}_\perp{}^2\ (\mathbf{q}_\perp{}^2+\lambda^2)^{-1}\int_0^1 dA\int_0^1 dx[A(1-A)]^{-1+\zeta}\{(1-\zeta)(\tfrac{1}{2}-A+A^2)(\tfrac{1}{2}-x+x^2)$$
$$\times[x(1-x)\mathbf{q}_\perp{}^2+m^2]^{-\zeta}+[\tfrac{1}{4}-\tfrac{1}{2}A(1-A)+x(1-x)A(1-A)]m^2\zeta[x(1-x)\mathbf{q}_\perp{}^2+m^2]^{-1-\zeta}\}$$

$$=m^{2\zeta}\pi\csc\pi\zeta\ [\Gamma(\zeta)]^2[\Gamma(2\zeta)]^{-1}\int_0^\infty d\mathbf{q}_\perp{}^2(\mathbf{q}_\perp{}^2+\lambda^2)^{-1}\int_0^1 dx\{\tfrac{1}{2}(1-\zeta^2)(1+2\zeta)^{-1}(\tfrac{1}{2}-x+x^2)[x(1-x)\mathbf{q}_\perp{}^2+m^2]^{-\zeta}$$
$$+\tfrac{1}{2}(1+2\zeta)^{-1}[\tfrac{1}{2}(1+\zeta)+\zeta x(1-x)]m^2\zeta[x(1-x)\mathbf{q}_\perp{}^2+m^2]^{-1-\zeta}\}$$

$$=\pi\zeta^{-1}\csc\pi\zeta\ [\Gamma(1+\zeta)]^2[\Gamma(2+2\zeta)]^{-1}\int_0^1 dx\{(1-\zeta^2)(\tfrac{1}{2}-x+x^2)\zeta^{-1}F(\zeta,1;1+\xi;1-x(1-x)\lambda^2/m^2)$$
$$+[\tfrac{1}{2}+\zeta(\tfrac{1}{2}+x-x^2)]\zeta(1+\zeta)^{-1}F(1+\zeta,1;2+\zeta;1-x(1-x)\lambda^2/m^2)\}\,, \quad \text{(B4)}$$

where F denotes the hypergeometric function.

Let ζ be small and positive, then it is sufficient to use in (B4)

$$F(\zeta,1;1+\zeta;z)\sim 1-\zeta\ln(1-z)-\zeta^2\sum_1^\infty z^n/n^2$$

and

$$F(1+\zeta,1;2+\zeta;z)\sim -z^{-1}\ln(1-z)\,. \quad \text{(B5)}$$

With (B5), (B4) gives that, for ζ small and positive

$$\bar{M}(\zeta)\sim\tfrac{1}{3}\zeta^{-3}[\Gamma(1+\zeta)]^2[\Gamma(2+2\zeta)]^{-1}\{1-\zeta[\ln(\lambda^2/m^2)-13/6]-\zeta^2$$
$$-\tfrac{1}{2}\zeta^2\int_0^1 dx[3-2\lambda^2m^{-2}x^3(1-2x)][1-x(1-x)\lambda^2/m^2]^{-1}\ln[x(1-x)\lambda^2/m^2]\}\,. \quad \text{(B6)}$$

A comparison of (B4) with (B6) gives that for large $|k^2|$ with fixed λ and m,

$$6|k^2|M(k^2)\sim[\ln(|k^2|/\lambda^2)]^2+\tfrac{1}{3}\ln(|k^2|/\lambda^2)+C\,, \quad \text{(B7)}$$

where

$$C=-[\ln(\lambda^2/m^2)]^2+(13/3)\ln(\lambda^2/m^2)-8/3-\pi^2/3-\int_0^1 dx\,[3-2\lambda^2m^{-2}x^3(1-2x)]$$
$$\times[1-x(1-x)\lambda^2/m^2]^{-1}\ln[x(1-x)\lambda^2/m^2]. \quad \text{(B8)}$$

APPENDIX C

In this appendix we rederive (5.10) in the manner of Appendix B. Similar to (B1), we have, as $\omega\to\infty$ with scalar photons,

$$\mathfrak{M}_{0L}{}^{(D)}\sim(2\pi)^{-3}i\omega e^6Z^2M_L(k^2)\,, \quad \text{(C1)}$$

where

$$M_L(k^2)=-2\pi^{-2}\int d\mathbf{q}_\perp\ (\mathbf{q}_\perp{}^2+\lambda^2)^{-2}\int d\mathbf{p}_\perp\int_0^1 dA\,|k^2|\{[\mathbf{p}_\perp{}^2+m^2+A(1-A)|k^2|]^{-2}$$
$$-[(\mathbf{p}_\perp+\tfrac{1}{2}\mathbf{q}_\perp)^2+m^2+A(1-A)|k^2|]^{-1}[(\mathbf{p}_\perp-\tfrac{1}{2}\mathbf{q}_\perp)^2+m^2+A(1-A)|k^2|]^{-1}\}$$
$$=2\int_0^\infty d\mathbf{q}_\perp{}^2\ (\mathbf{q}_\perp{}^2+\lambda^2)^{-1}|k^2|\int_0^1 dA\int_0^1 dx\,x(1-x)A^2(1-A)^2[x(1-x)\mathbf{q}_\perp{}^2+m^2+A(1-A)|k^2|]^{-2}. \quad \text{(C2)}$$

Mellin transformation with respect to $|k^2|$ then yields

$$\bar{M}_L(\zeta)=\int_0^\infty d|k^2|\,(|k^2|/m^2)^{-\zeta}M_L(k^2)$$
$$=2m^{2\zeta}\pi(1-\zeta)\csc\pi\zeta\int_0^\infty d\mathbf{q}_\perp{}^2(\mathbf{q}_\perp{}^2+\lambda^2)^{-1}\int_0^1 dA\int_0^1 dx\,x(1-x)[A(1-A)]^\zeta[x(1-x)\mathbf{q}_\perp{}^2+m^2]^{-\zeta}$$
$$=2\pi(1-\zeta)\csc\pi\zeta\,[\Gamma(1+\zeta)]^2[\Gamma(2+2\zeta)]^{-1}\zeta^{-1}\int_0^1 dx\,x(1-x)F(\zeta,1;1+\zeta;1-x(1-x)\lambda^2/m^2). \quad \text{(C3)}$$

Let ζ be small and positive so that (B5) can be used. Then

$$\bar{M}_L(\zeta)\sim 2\zeta^{-2}(1-3\zeta)\int_0^1 dx\,x(1-x)\{1-\zeta\ln[x(1-x)\lambda^2/m^2]\}\sim\tfrac{1}{3}\zeta^{-2}\{1-\zeta[\ln(\lambda^2/m^2)+\tfrac{4}{3}]\}. \quad \text{(C4)}$$

Accordingly, the desired answer is that, for large $|k^2|$ but fixed nonzero values of m and λ,

$$M_L(k^2)\sim\tfrac{1}{3}|k^2|^{-1}[\ln(|k^2|/\lambda^2)-\tfrac{4}{3}]. \quad \text{(C5)}$$

Note again that m does not appear in (C5).

PHYSICAL REVIEW VOLUME 183, NUMBER 5 25 JULY 1969

Coupled Dynamical Equations Incorporating Unitarity and Crossing. I. $\pi\pi$ and πK Scattering*

STEPHEN HUMBLE
Department of Physics, University of Colorado, Boulder, Colorado 80302
(Received 17 February 1969)

An equation proposed by Zimmermann, which takes account of the normal thresholds in s, t, and u channels, is generalized to two-body reactions involving particles of any spin or isospin, and extended to include a number of coupled processes in each channel. In this form, the resulting equations, besides satisfying the requirements of low-energy unitarity and crossing symmetry, take some account of the effect of all reactions in each channel, as well as the detailed energy-dependent effects of one or two low-mass processes. The coupled $\pi\pi$ and πK system is considered, and approximate solutions are found which give the ρ and K^* resonance parameters within 15% of the accepted experimental values, as well as a κ resonance in the $I=\frac{1}{2}$ s-wave πK partial wave. The $\pi\pi$ s-wave phase shifts in this case are found to be very negative, decreasing rapidly to $-\pi$; but with the coupling of the $\pi\pi\to\pi\omega$ reaction to this system; a solution is obtained giving an $I=0$, $\pi\pi$ s-wave which, at low energies, is in agreement with some recent phenomenological analyses.

I. INTRODUCTION

THE development of S-matrix theory based upon the requirements of Lorentz invariance, unitarity, analyticity, and crossing has been a very powerful tool in understanding the strong interactions of fundamental particles. In principle, it is able to predict the scattering amplitude for any hadron reaction, and it has been suggested that the simultaneous determination of these amplitudes, coupled via the unitarity and crossing conditions, could be made with only the input of an over-all scale. Such complete solutions, however, are clearly impossible to calculate, since they involve the solution of an infinite number of coupled channels. Nevertheless, it has been hoped that approximate low-energy solutions could be found which at least reflect the physical situation on the assumption that the effects of the higher-mass processes are either negligible or can be inserted phenomenologically.

Most of the work in this direction has concentrated on the solution of dispersion relations which stress the cut-plane analyticity of the scattering amplitudes, with the corresponding discontinuities given by the unitarity conditions. Unfortunately, whether one uses the full Mandelstam representation[1] or the multichannel N/D partial-wave equations of Bjorken,[2] the

* Supported by Air Force Office of Scientific Research, Office of Aerospace Research, U. S. Air Force, under Grant No. AF-AFOSR-30-67.

[1] S. Mandelstam, Phys. Rev. 112, 1344 (1958).
[2] J. D. Bjorken, Phys. Rev. Letters 4, 473 (1960).